

Structural Analysis of Small Molecule Binding to the BAZ2A and BAZ2B Bromodomains

Dr. Andrea Dalle Vedove,^[a] Dr. Dimitrios Spiliotopoulos,^[b] Dr. Vito G. D'Agostino,^[a] Dr. Jean-Rémy Marchand,^[b] Dr. Andrea Unzue,^[c] Prof. Cristina Nevado,^[c] Dr. Graziano Lolli,^{*,[a]} and Prof. Amedeo Caflisch^{*,[b]}

[a] Centre for Integrative Biology
University of Trento
via Sommarive 9, 38123, Povo-Trento, Italy
E-mail: graziano.lolli@unitn.it

[b] Department of Biochemistry
University of Zürich
Winterthurerstrasse 190, CH-8057, Zürich, Switzerland
E-mail: caflisch@bioc.uzh.ch

[c] Department of Chemistry
University of Zürich
Winterthurerstrasse 190, CH-8057, Zürich, Switzerland

Supporting information for this article is given via a link at the end of the document.

Abbreviations: BAZ2A, bromodomain adjacent to zinc finger domain protein 2A; BAZ2B, bromodomain adjacent to zinc finger domain 2B; EZH2, Enhancer of Zest Homolog 2; BET, bromodomain and extra terminal; Kac, acetyllysine; PCa, prostate cancer.

Abstract: The bromodomain-containing protein BAZ2A is a validated target in prostate cancer, while the function of its paralog BAZ2B is still undefined. The bromodomains of BAZ2A and BAZ2B have a very similar binding site for their natural ligand, the acetylated lysine side chain. Here, we present an analysis of the binding modes of eight compounds belonging to three distinct chemical classes. For all compounds, the moiety mimicking the natural ligand makes essentially identical interactions in the BAZ2A and BAZ2B bromodomains. In contrast, the rest of the molecule is partially solvent exposed and shows different orientations and interactions in the two bromodomains. Some of these differences could be exploited for designing selective inhibitors within the BAZ2 bromodomain subfamily.

The bromodomain of BAZ2B shares with its paralog BAZ2A a very similar Kac-binding site (76% sequence identity and 93% similarity). The physiological function of BAZ2B is still unknown, while single nucleotide polymorphisms in the BAZ2B gene locus have been associated with sudden cardiac death [5].

First fragment binders for BAZ2B have been identified by Ciulli and coworkers in 2013 [6]. In contrast to the members of the BET (bromo and extraterminal domain) subfamily of human bromodomains for which many potent and selective inhibitors have been developed (with 11 of them currently being tested in clinical trials [4]), the BAZ2 bromodomains have a shallow Kac binding pocket with only two potent inhibitors developed so far, unable to discriminate between the two paralogs [7-8].

Here we report eight crystallographic structures of small molecules from three different chemical classes in complex with the BAZ2A bromodomain; structures for seven of these molecules were also determined in complex with the bromodomain of BAZ2B. Comparison of those structures has allowed the identification of common and divergent features in the binding modes of fragments/small molecules to the two BAZ2 bromodomains, providing additional hints for the development of specific BAZ2A or BAZ2B bromodomain inhibitors. Additionally, one of the BAZ2A structures derives from a novel crystallographic packing and space group and was determined at a resolution of 1.1 Å, constituting the highest resolution structure for this bromodomain determined to date.

Introduction

Bromodomains are epigenetic reader modules that recognize acetylated lysines (Kac) in histones and other proteins; they are associated with additional domains involved in chromatin remodeling and transcriptional regulation (histone acetylases, methyltransferases, transcription factors and helicases) [1].

Bromodomain adjacent to zinc finger domain protein 2A (BAZ2A) is over-expressed in prostate cancer (PCa), inducing aberrant gene silencing [2]. BAZ2A expression correlates both with PCa aggressiveness and recurrence and with the evolution of a metastatic phenotype. Invasion and migration of metastatic PCa cells are drastically impaired upon BAZ2A knockdown. The chromatin template activities of BAZ2A mediate its oncogenic effects, making its bromodomain a promising target to interfere with PCa progression and recurrence. BAZ2A induces aberrant gene silencing in prostate cancer also cooperating with Enhancer of Zest Homolog 2 (EZH2), whose altered expression is linked to malignancy and poor prognosis [3]. Three EZH2 inhibitors are currently being tested in clinical trials [4].

Results and Discussion

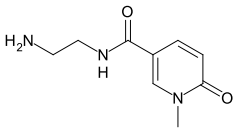
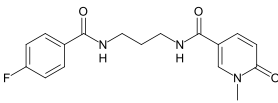
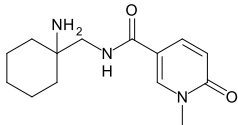
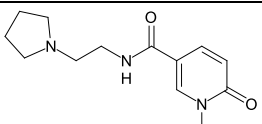
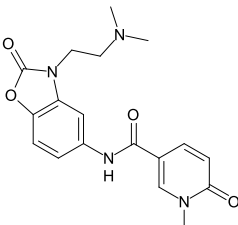
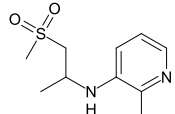
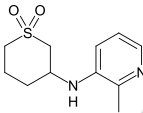
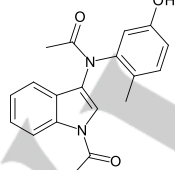
The eight small molecules selected for structural studies in complex with BAZ2A and BAZ2B belong to three different chemical classes (Table 1). The 1-methylpyridinone bearing compounds **1-5** were prioritized following *in silico* screening and competition binding assays, starting from a parent fragment identified in a previous screening campaign [9]. The 3-amino-2-methylpyridine derivatives **6-7** and the acetyl-indole compound **8**

FULL PAPER

had been identified previously as BAZ2B ligands and represent interesting molecules for further optimization of their potency and selectivity [10-11]. We first present the results of a substructure

search (from fragment 1 of ref. 8) followed by a comparison of the binding sites of BAZ2A and BAZ2B, and then we analyze differences in binding modes and interaction motifs.

Table 1. Binding activity for compounds 1-8.

Compound	Structure	BAZ2A				BAZ2B			
		% Ctrl ^a	IC ₅₀ ^b (μM)	K _D ^c (μM)	PDB	% Ctrl ^a	IC ₅₀ ^b (μM)	K _D ^c (μM)	PDB
1		73	> 820	> 400	6FG6	59	> 1000	-	6FH6
2		84	> 1000	110	6FGF	90	> 1000	-	6FH7
3		> 90	-	-	6FGV	68	-	-	6FGT
4		57	-	-	6FGW	69	-	-	6FGU
5		25	88	17	6FGG	19	89	-	-
6		21	-	-	6FGH	7	> 500 ^d	-	5L96
7		21	-	-	6FGI	4	279 ^d	-	5L8T
8		42	24	-	6FGL	29 ^a 54 ^e	8	23 ^f	5E73

Dashes indicate data not acquired. ^a Residual binding of the H3K(Ac)14 peptide at 1 mM compound concentration measured by AlphaScreen; lower percentage values indicate tighter binding of compound. ^b Determined by Alphascreen. ^c Determined by BROMOscan. ^d Reported in reference [10], by Alphascreen. ^e Residual binding at 0.05 mM measured by AlphaScreen in reference [11]. ^f Reported in reference [11], by BROMOscan. Compounds 6 and 7 were tested as racemic mixtures.

Substructure search

With the aim of increasing specificity for BAZ2A versus BAZ2B, we performed a substructure search using the *N*-methyl-2-pyridone-5-carboxamide head (from fragment 1 of ref. 8) as a query on the ZINC15 database. This search yielded 444 compounds that include a positively charged, H-bond donor, or halogen-bond donor tail, as to reach BAZ2A Glu1820 side chain (whose corresponding residue is Leu1891 in BAZ2B). These compounds were docked to the BAZ2A structure from the complex with fragment 1 of ref. 8 (PDB 5MGJ) using the program SEED [12-13]. In all BAZ2A structures available at the time, Glu1820 adopted the mm rotamer ($\chi = -65^\circ$). On the other hand, we noticed that this residue is not involved in any intramolecular interactions and changed it for docking to the pt rotamer ($\chi = 63^\circ$), which points towards the interior of the cavity, emulating an induced fit. Charged compounds were ranked according to the electrostatic energy while uncharged compounds according to consensus scoring as in our previous work (see Methods). A total of 22 compounds (14 with a positively charged amino group and 8 non-charged) were selected and tested for BAZ2A binding at single dose in the AlphaScreen assay (Table S1). Dose response curves of the most active compounds were then obtained using the AlphaScreen assay and/or the BROMOScan assay (Table 1 and Fig. S1 and S2). Compound 5 is the most active against the BAZ2A bromodomain in both assays with an IC_{50} value of 88 μ M and a K_D of 17 μ M. It has been reported by several groups that the K_D values measured by the BROMOScan assay are up to an order of magnitude more favorable than the IC_{50} values obtained by AlphaScreen [14-17]. Overall, the substructure search resulted in five new crystal structures but only a modest improvement of affinity with respect to the original hit (from a K_D of 51 μ M for fragment 1 of ref. 8 to a K_D of 17 μ M for ligand 5 in this work).

The structure of the bulky compound 5 could not be determined in complex with BAZ2B; packing constraints impeded binding of the compound by soaking, while co-crystallization yielded no crystals. In contrast, binding of the compound in BAZ2A induced a new crystallographic packing through the stacking of two symmetry-related 2-benzoxazolinone moieties bound to two neighboring protein chains (Fig. S3). The X-ray structure was determined at a 1.1 Å resolution, which represents the highest resolution structure for the BAZ2A bromodomain so far. The new orthorhombic crystallographic packing has no influence on the pose of compound 5, as a very similar binding mode was observed in the significantly lower resolution structure (3.0 Å, not shown) which was obtained by soaking the compound in the usual trigonal crystal form. The only difference resides in the highly-degraded electron density for the terminal *N,N*-dimethylethylamine group in the lower resolution structure. The slightly higher affinity of compound 5 with respect to the other 1-methylpyridinone derivatives 1-4 can be explained by the T-shaped π - π stacking interaction between the 2-benzoxazolinone ring and Trp1816 (Fig. 1). Moreover, the *N,N*-dimethylamine substituent of compound 5 is involved in additional van der Waals interactions with the aforementioned tryptophan residue, while the non-optimal geometry makes questionable whether a cation- π interaction between the same groups also favorably contributes to the binding energy. The terminal dimethylamine is also in close proximity to Glu1878, which would need to switch to a different conformer in order to establish an ionic interaction; such a rearrangement is not observed and Glu1878 remains involved in

the intramolecular electrostatic interaction with Lys1881, as observed in the other BAZ2A structures.

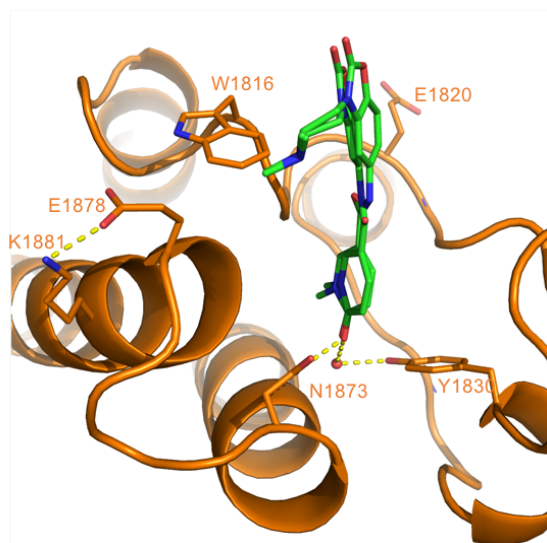


Figure 1. Binding mode of compound 5. The amide linker of compound 5 (green) can assume two conformations in the BAZ2A pocket.

Comparison of BAZ2A and BAZ2B binding sites

The holo structures of BAZ2A and BAZ2B here presented show common features irrespective of the bound inhibitor. The Kac-binding sites have similar parallelepiped-like shape largely defined by the ZA loop (residues 1813-1838 and 1884-1909 in BAZ2A and BAZ2B, respectively) and BC loop (residues 1873-1877 and 1944-1948 in BAZ2A and BAZ2B, respectively). In complexes with different ligands, the BAZ2A bromodomain shows no significant structural deviations in the loops. Upon superposition over all C_α atoms the maximal pairwise rmsd is 0.56 Å for C_α atoms in the BC loop and 0.70 Å for C_α atoms in the ZA loop (Fig. 2a). In BAZ2B structures, a larger flexibility is observed for the ZA loop while the BC loop, similarly to BAZ2A, shows limited positional variability (max pairwise rmsd of 0.44 Å for C_α atoms in the BC loop and 1.34 Å for C_α atoms in the ZA loop, Fig. 2b). The plasticity of the ZA loop emerges also from the structural overlap of the two bromodomains with a deviation as large as 1.8 Å between the C_α atoms of Leu1826 in BAZ2A and the corresponding BAZ2B Leu1897 residue (in complex with compound 8, PDB codes 6FGL and 5E73) while the largest deviation in the BC loop is smaller than 1.0 Å (Fig. 2c). The higher disorder of the ZA loop in BAZ2B might originate, at least in part, from the presence of Pro1824 in BAZ2A whose corresponding residue is Leu1895 in BAZ2B. On the other hand, the crystal packing could differently influence loops flexibility in the two bromodomains, an effect that is difficult to weight accurately.

BAZ2A seems to have a reduced aperture of the binding site with respect to BAZ2B if one considers distances between corresponding pairs of backbone atoms in the two loops. However, a more detailed analysis reveals that the effective space available to the ligand is essentially identical in the two bromodomains, since the distance between the two side chains that protrude from the two loops to the center of the binding site is in both cases about 8.3 Å, as measured between the tip of the gatekeeper side chain and the ZA loop Val1827 or Val1898 (in BAZ2A or BAZ2B, respectively, Fig. 2c).

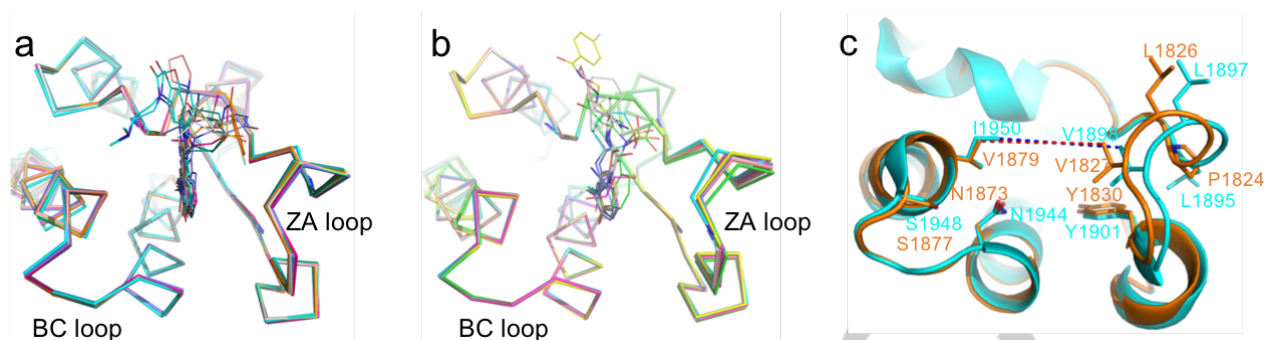


Figure 2. Flexibility and structural variations in BAZ2A and BAZ2B bromodomains

- Superposition of BAZ2A structures in complex with compounds **1-8** (Table 1) shows limited variability in the BC and ZA loops.
- Superposition of BAZ2B structures in complex with compounds **1-4** and **6-8** shows higher flexibility of the ZA loop.
- Binding site aperture and distances of main interaction motifs in BAZ2A and BAZ2B bromodomains. BAZ2A (orange, PDB 6FGL) and BAZ2B (cyan, PDB 5E73) structures deviate significantly from each other at the tip of the ZA loop (Leu1826 in BAZ2A and Leu1897 in BAZ2B); superposition is shown for structures in complex with compound **8**. The substitution of Pro1824 in BAZ2A to Leu1895 in BAZ2B could play a role in the observed divergence as well as in the larger flexibility of the loop in BAZ2B. Another relevant difference in the Kac pocket of the two bromodomains resides in the gatekeeper residue, Val1879 in BAZ2A and Ile1950 in BAZ2B. Aperture of the binding site is similar in the two bromodomains as shown by the dashed lines connecting the tip of the side chains of the gatekeeper residue and the opposite valine (Val1879-Val1827 indicated by a red dashed line for BAZ2A, and Ile1950-Val1898 indicated by a blue dashed line for BAZ2B).

Comparison of binding modes

In the deepest part of the pocket, i.e., the one that recognizes the acetyl moiety of Kac, the acetyl oxygen forms hydrogen bonds with the side chains of the evolutionary conserved Asn1873 and Tyr1830 in BAZ2A (Asn1944 and Tyr1901 in BAZ2B), the latter interaction involving a structurally conserved water molecule (W1) acting as a bridge. Both hydrogen bonds are present in all crystal structures of BAZ2A/B reported in this work as well as in those disclosed previously with the exception of the complex between BAZ2B and 6-hydroxyindole in which the NH of the ligand replaces the water W1 (PDB code 5E9I) [18]. The scatter plot in Fig. 3a shows that the distance to the bridging water is shorter than the distance to the side chain of the conserved asparagine for all compounds (except for the acetyl-indole derivative **8**) in agreement with previous reports [14,

19-20]. Interestingly, the hydrogen bond distances can be clustered on the basis of the compounds chemical class independently of the bound bromodomain. The distance to the structurally conserved water reflects the degree of burial of the compounds (Fig. 3b). The 1-methylpyridinone compounds **1-5** bind deeper in the Kac pocket in comparison to compounds from the other chemical classes. The hydrogen bond distance to the side chain NH₂ of the conserved Asn is relatively large (3.2 to 3.5 Å) for the ligands with an aromatic nitrogen atom (pyridine) acting as hydrogen bond acceptor (compounds **6**, **7**, and the ligands in 5OR9 and 5ORB) while it is significantly shorter (2.7 to 3.0 Å) for all other compounds which have a carbonyl oxygen as acceptor as well as for the hydroxyl oxygen of 1,2-ethanediol in BAZ2A (PDB 4LZ2).

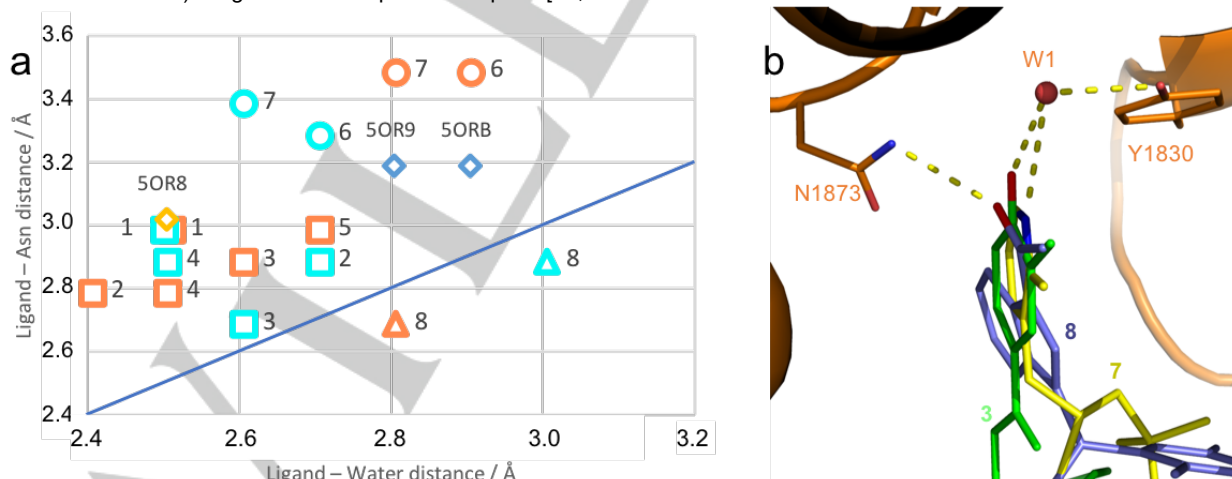


Figure 3. Binding modes in the acetyl-recognizing region of BAZ2A and BAZ2B Kac pockets.

- Scatter plot of the hydrogen bond distances between compounds **1-8** (Table 1) and the conserved asparagine (Asn1873 in BAZ2A and Asn1944 in BAZ2B) and water molecule at the bottom of the Kac pocket of the two bromodomains. Numbers denote the ligand, symbols denote the chemical class (square for 1-methylpyridinone compounds **1-5**, circle for 3-amino-2-methylpyridine derivatives **6-7**, and triangle for the acetyl-indole **8**), and color the bromodomain (orange and cyan for BAZ2A and BAZ2B, respectively). Distances for the 1,3-dimethyl-benzimidazolone (5OR8 in complex with BAZ2A, light-orange diamond) and the two 1-methyl-cyclopentapyrazole derivatives (5ORB and 5OR9, in complex with BAZ2B, blue diamonds), which were recently described [29], are also included. Note that compounds **6**, **7**, and the ligands in 5ORB and 5OR9 have a nitrogen atom in an aromatic ring as hydrogen bond acceptor while all other compounds have a carbonyl oxygen atom.
- Hydrogen bond pattern at the bottom of the BAZ2A Kac pocket is represented for the different chemical classes. 1-methylpyridinone (compound **3**, green) and 3-amino-2-methylpyridine (compound **7**, yellow) derivatives form a hydrogen bond with the conserved water molecule W1; the acetyl-indole derivative **8** (purple) is closer to Asn1873 than to W1.

In the middle part of the cavity, the difference in the gatekeeper Val1879 in BAZ2A to Ile1950 in BAZ2B imposes a tilting of the aromatic ring constituting the head group of the various molecules reported here. The influence of the gatekeeper residue on the orientation of small-molecule ligands in the Kac binding site has been already reported [11]. The observed tilting is only about 10 degrees in compounds **6-7** that bear the small 2-

methylpyridine head group (Fig. 4a), where the anchoring nitrogen atom is part of the aromatic ring (a pyridine), and more pronounced (between 15 and 25 degrees, depending on the inhibitor, Fig. 4b) in the case of the more protruding and larger 1-methylpyridinone and acetyl-indole head groups in compounds **1-4** and **8**, respectively.

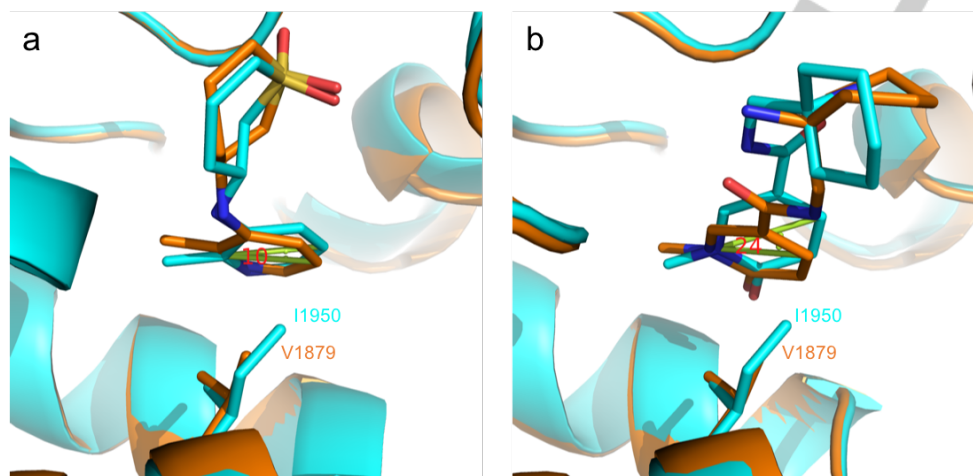


Figure 4. Tilting of the compounds head group induced by the different gatekeeper residues varies with the chemical scaffold of the ligand.

- Head group in compound **7** tilts by only 10° in BAZ2B (cyan) with respect to BAZ2A (orange). The angle of the aromatic planes is shown by two segments (green with angle value in red).
- Tilting is more pronounced in compound **3** (24°). Colour code same as above.

The largest difference in BAZ2A/B binding are observed for the tail moiety, as evident for compounds **1**, **2**, and **8** (Fig. 5). In BAZ2B, the ethyldiamine tail of compound **1** closely follows the route of the Kac residue in histone peptides bound to BAZ2A and BAZ2B (PDB 4QBM, 4QC1 and 4QC3) [21]; in BAZ2A, the same tail is rotated by about 60° and close to Trp1816 and Pro1817 of the WPF shelf (Fig. 5a). The divergence can be exacerbated by differences in sequence and structure between BAZ2A and

BAZ2B in the more external part of the Kac binding pocket. Compound **2** binds to BAZ2A with its fluorophenyl tail in hydrophobic contact with Leu1826 at the tip of the ZA loop (Fig. 5b). In BAZ2B, the tail is rotated by about 180° and the fluorophenyl moiety is in contact with Leu1891, corresponding to Glu1820 in BAZ2A. The crystallographic packings do not influence the orientation of compound **2** in both bromodomain structures.

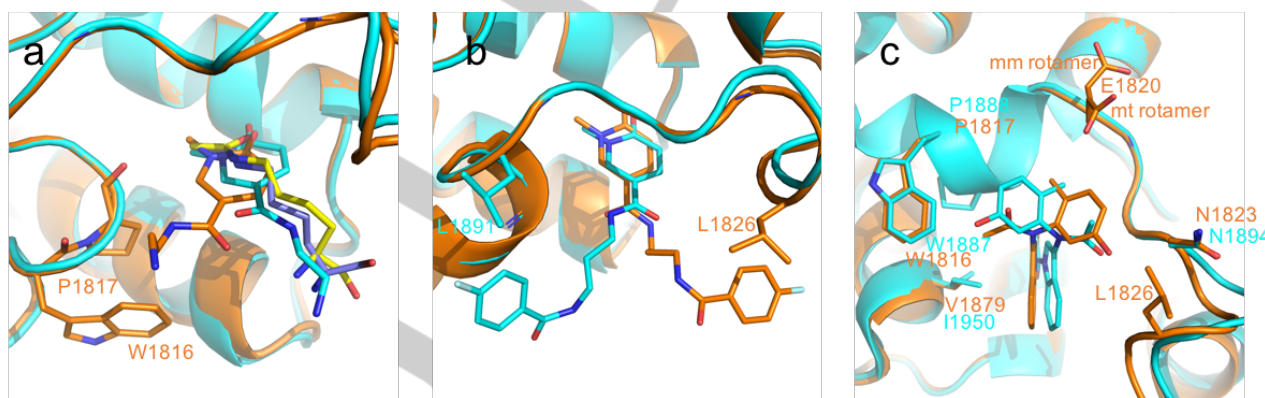


Figure 5. Similar binding modes of head groups to BAZ2A (orange) and BAZ2B (cyan) and differences in the tail groups.

- The binding mode of compound **1** to BAZ2B is similar to that of Kac to BAZ2A (PDB 4QBM, yellow) and BAZ2B (4QC1, purple). The tail of compound **1** is oriented differently in BAZ2A and BAZ2B.
- The tail of compound **2** orients in opposite directions in BAZ2A and BAZ2B.
- Positions of the two substituents in compound **8** are inverted in BAZ2A and BAZ2B. The side chain of Glu1820 in BAZ2A is present in double conformation assuming the mm and mt rotamers.

Compound **8** shows substantial differences in its binding mode to the two BAZ2 bromodomains (Fig. 5c). The 3-amino-1-acetyl-indole head group is tilted due to the difference in the gatekeeper residue. The head group bears two additional substituents on the nitrogen in position 3, which are different in size, a small acetyl group and a bulkier 2-methyl-5-

hydroxybenzene ring. The two substituents are oriented in opposite directions in the two bromodomains. In BAZ2A the smaller gatekeeper Val1879 keeps the acetyl-indole ring close to the WPF shelf so that the acetyl group is in van der Waals contact with Trp1816 and Pro1817, whereas the 2-methyl-5-hydroxybenzene ring is oriented towards Asn1823 and Leu1826

on the tip of the ZA loop. In BAZ2B the gatekeeper Ile1950 pushes the acetyl-indole ring away from the WPF shelf; the 2-methyl-5-hydroxybenzene ring is now in contact with Trp1887 and Pro1888 while the acetyl group occupies the reduced space (in comparison with BAZ2A) towards the tip of the ZA loop also forming a hydrogen bond with main chain nitrogen of Asn1894.

Selectivity filters in BAZ2A

Two variations in sequence between BAZ2A and BAZ2B, Val1879 to Ile1950 (Fig. 4, the gatekeeper residue) and Glu1820 to Leu1891, are putative selectivity determinants which were not fully explored by the compounds reported here. In spite of interesting differences in their binding modes to BAZ2A and BAZ2B, similar affinity for both bromodomains were measured for all tested compound (Table 1 and S1).

For ligands **1-4**, tails are involved in a limited number of contacts with the protein matrices; moreover, the electron density rapidly degrades moving towards the more external part of the inhibitors, indicating high flexibility and possible multiple conformations for these tails. The positively charged tails of compounds **1**, **3** and **4** in BAZ2A are correctly oriented towards Glu1820 (Leu1891 in BAZ2B), but are too flexible and short to be involved in electrostatic interactions (Fig. 6). Nevertheless, they represent interesting vectors to explore this difference in sequence. The tail of compound **5** contacts residues that are conserved between the two bromodomains and the binding mode in BAZ2B would be probably similar to that observed in BAZ2A (Fig. 1). In BAZ2A, the positively charged tail of ligand **5** is oriented towards Glu1878 and thus points in the opposite direction with respect to the side chain of Glu1820. Substitutions in different positions of an aromatic ring that acts as spacer (like the 2-benzoxazolinone of compound **5**) could prove useful in correctly reorienting a terminal positively charged group towards Glu1820 while keeping the π - π stacking interaction with Trp1816.

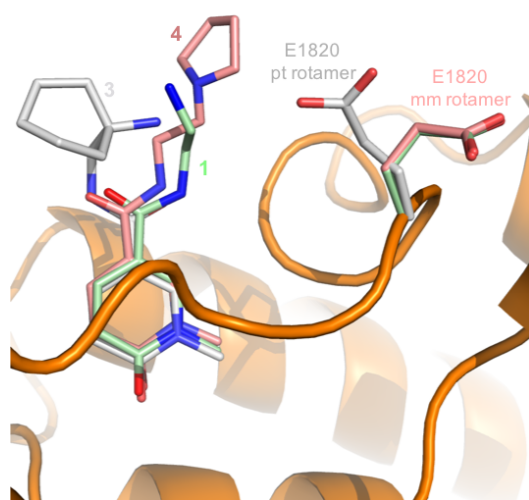


Figure 6. Orientations of ligand tail groups in BAZ2A and the Glu1820 side chain. Compounds **1**, **3**, and **4** (light green, gray, and pink, respectively) bind to BAZ2A with different orientations of the tail groups. In the complex with compound **3**, Glu1820 assumes the pt rotameric state (gray).

Compounds **6** and **7** show very similar binding modes in the two bromodomains (Fig. 4a). Despite containing a stereogenic center, a single enantiomer is present or at least largely predominant in the X-ray structures in complex with BAZ2B [10]. The lower resolution of the BAZ2A crystallographic structures

makes questionable whether a similar specificity is possible also for this bromodomain, where the smaller gatekeeper residue could result in a less stringent enantiomeric selectivity, a possibility worth further investigation.

In compound **8**, the bipartite tail assumes inverted orientations in the two bromodomains as a consequence of the differential tilt imposed to the inhibitor by the gatekeeper residues. Asymmetry and bulkiness of the two substituents of the tail could then be exploited in order to gain selectivity for BAZ2A, as well as appropriate functional groups to complement the different charge distribution of the bromodomains; in BAZ2A, the 2-methyl-5-hydroxybenzene substituent is close to Glu1820 (Fig. 5c).

Finally, the side chain of Glu1820 in BAZ2A can assume conformations others than the mm rotamer reported so far. In the complexes with compounds **3** and **8**, Glu1820 is present as pt rotamer (the one selected in the protein model used in the docking procedure) and mt rotamer, respectively (Fig. 5c and 6). Both pt and mt rotamers point towards the interior of the binding cavity, providing evidence that the interaction with Glu1820 can be exploited as a specificity determinant for small molecules binding to BAZ2A versus BAZ2B.

Conclusions

We present eight new structures of the BAZ2A bromodomain in complex with small molecules that originate from the expansion of fragment hits identified by docking. While the BAZ2A/B ligands **6-8** were reported previously [10-11], compounds **1-5** are disclosed here for the first time. They are derivatives of the *N*-methyl-2-pyridone-5-carboxamide head (i.e., fragment **1** of Ref. 8) which were identified by substructure search and docking with evaluation of binding energy using a force field energy with electrostatic desolvation effects. Compound **5** showed a slightly better binding affinity to BAZ2A with respect to compounds **1-4** and to the parent fragment (**1** of Ref. 8). The complex with compound **5** was determined in a new space group and crystallographic packing and constitutes the so far highest resolution structure for the BAZ2A bromodomain. The eight holo structures of BAZ2A supplement the seven structures already deposited in the PDB (viz., apo, the complex with the acetylated H4 peptide, and five complexes with fragments/small molecules) and together constitute a large dataset for a detailed description of small molecules binding to the Kac binding site of BAZ2A.

We focused the analysis on the comparison with the very similar pocket of the cognate BAZ2B bromodomain for which many holo structures are available in the PDB. Structures of seven small molecules are available in complex with both bromodomains (four of them in complex with BAZ2B also reported here for the first time). Four main observations emerge from the comparative analysis. First, the slightly lower flexibility observed for the ZA loop in BAZ2A is likely due to the presence of Pro1824 whose corresponding BAZ2B residue is Leu1895. Second, in the deepest part of the pocket residues are conserved between the two bromodomains and the anchoring of the head group is largely related to its chemical identity and shape. Third, the difference in the gatekeeper residue induces a tilting of the head group (acetyl-lysine mimic) which can influence the orientation of the substituents (e.g., compound **8**, Fig. 5c). Fourth, the BAZ2A Glu1820 side chain (whose corresponding BAZ2B residue is Leu1891) can assume rotameric configurations directing its

negative charge towards the Kac pocket which suggests that this residue can be exploited as a specificity determinant for small molecules binding to BAZ2A versus BAZ2B.

Experimental Section

Substructure search, docking and ranking

A library of 444 molecules was obtained by substructure search using the *N*-methyl-2-pyridone-5-carboxamide (the head of compound **1** of Ref. 8) as query on the ZINC15 database. Compounds that did not include a positively charged or H-bond or halogen-bond donor tail, theoretically capable of reaching BAZ2A Glu1820 side chain, or that presented unwanted substitutions on the head group (i.e., in position 6) were discarded. The molecular weight of these molecules ranges from 166.1 to 412.2 g/mol with a median of 252.2 g/mol. The number of rotatable bonds ranges from 1 to 12 with a median of 4. The number of hydrogen bond donors and acceptors ranges from 0 to 3 with a median of 1 and from 1 to 6 with a median of 4, respectively.

For each of the 444 derivatives (96 with a positively charged amino group and 348 non-charged) of *N*-methyl-2-pyridone-5-carboxamide, 100 conformers were generated relying on the RDKit [22] and parametrized using CGenFF [23–24]. The program SEED [12–13] was employed for docking to the BAZ2A structure (PDB 5MGJ with Glu1820 in the *pt* rotameric configuration) a total of 44400 conformers. The poses of the charged compounds were ranked according to the electrostatic interaction energy with approximation of solvent screening effects by the generalized-Born model with numerical evaluation of the Born radii [25]. The uncharged molecules were ranked according to consensus scoring using the median rank of three energy terms as in our previous work [9] with the difference that the van der Waals efficiency was counted twice, i.e., weighted two times with respect to each of the two remaining terms, viz., electrostatic difference and SEED total energy. Double-weighting the van der Waals efficiency favors small molecules with a small number of non-hydrogen atoms.

Compound Purity.

Compounds **1–7** were purchased from Enamine. Compound **8** was synthesized as previously described [11]. The purity of the molecules was analyzed by HPLC-MS and NMR and is $\geq 95\%$.

Protein Expression and Purification

BAZ2AA-c002 was a gift from Nicola Burgess-Brown (Addgene plasmid #53623). For crystallization purposes, BAZ2A (aa. 1796–1899) and BAZ2B (aa. 1858–1972) bromodomains were produced as previously described [9]. Briefly, proteins were purified by IMAC, followed by buffer exchange, tag removal by TEV protease, a second IMAC and a size-exclusion chromatography. For the AlphaScreen assay, bromodomains were left with the 6×His-tag and then subjected to size-exclusion chromatography, using a Superdex 75 column, immediately after the first purification step by IMAC.

AlphaScreen Assay

Recombinant His tagged BAZ2A and BAZ2B bromodomains were tested by alpha technology in the presence of a biotinylated histone H3 acetylated lysine 14 peptide (H3K(Ac)14), H-YQTARKSTGGK(Ac)APRKQLATKAK(Biotin)-

OH) [26] using the AlphaScreen Histidine detection kit (Perkin Elmer). The assays were performed in 384 optiplates (Perkin Elmer) as already described [27] using equimolar amount of ligands at hooking point (750 nM) evaluated after 1 hr incubation at room temperature in buffer A (50 mM HEPES pH 7.4, 100 mM NaCl, 0.1% BSA, 0.05% CHAPS). Compounds, dissolved in DMSO, were tested in duplicate or dose-response and IC50 values were obtained by nonlinear regression of log(dose)-response fit using GraphPad Prism software. DMSO was kept below 2% as final concentration and data were normalized against corresponding DMSO controls.

BROMOscan Assay

Assays were performed at DiscoverX with the BROMOscan profiling service. BROMOscan is a competition-based technology using a ligand immobilized to a solid support and DNA-tagged bromodomains. Bromodomains are incubated with the ligand in the presence and absence of the putative inhibitors and eluted to be quantified by qPCR. Small molecules inhibiting the bromodomain binding to the immobilized ligand will reduce the amount of bromodomain captured and thus the qPCR signal [28]. The ligand used for the assay is proprietary and undisclosed. Dissociation constants (K_D) were calculated by fitting a 12-point dilution curve with starting concentration in the range 0.2–0.4 mM (depending on compound solubility) and a dilution factor of 3.0. All dose-responses were measured in duplicates.

Crystallization, Data Collection and Structure Solution

Co-crystallization of BAZ2A with the compounds of interest and crystallization and soaking for the BAZ2B bromodomain were performed as previously described [29]. Compounds were dissolved in crystallization or soaking solutions devoid of DMSO, which does bind in the Kac pocket of bromodomains [18, 30].

Diffraction data were collected at the Elettra Synchrotron Light Source (Trieste, Italy), XRD1 beamline (PDB 6FG6, 6FGF, 6FGG, 6FGH, 6FGI, 6FGL, 6FGT, 6FGU, 6FGV and 6FGW) and at the Swiss Light Source, Paul Scherrer Institute (Villigen, Switzerland), beamline PXI (PDB 6FH6 and 6FH7). Data were processed with XDS [31] and Aimless [32]; high resolution cutoff was selected according to Karplus and Diederichs [33]. BAZ2B crystals soaked with compounds **1** and **2** (PDB 6FH6 and 6FH7) were strongly anisotropic: ellipsoidal diffraction data were treated making use of the STARANISO server (<http://staraniso.globalphasing.org/cgi-bin/staraniso.cgi>). Structures were solved by molecular replacement with Phaser [34] using PDB 4IR5 as search model for BAZ2B and PDB 5MGJ for BAZ2A. Initial models were refined alternating cycles of automatic refinement with either Phenix [35] and manual model building with COOT [36].

Data collection and refinement statistics are reported in Table S2 and S3. Electron densities are shown in Fig. S4 for compounds **1–8** in all structures reported here.

Accession Codes

BAZ2A structures were deposited to the PDB with accession numbers 6FG6 (compound **1**), 6FGF (compound **2**), 6FGV (compound **3**), 6FGW (compound **4**), 6FGG (compound **5**), 6FGH (compound **6**), 6FGI (compound **7**), and 6FGL (compound **8**). BAZ2B structures were deposited to the PDB with accession numbers 6FH6 (compound **1**), 6FH7 (compound **2**), 6FGT (compound **3**), and 6FGU (compound **4**). Atomic coordinates and

experimental data will be released upon article publication.

ASSOCIATED CONTENT

The Supporting Information contains:

Supplementary Tables: 2D structures of all 1-methylpyridinone compounds and their binding-competition activities on BAZ2A measured by AlphaScreen in single dose; X-ray data collection and refinement statistics.

Supplementary Figures: AlphaScreen/BROMOscan dose-response curves for the selected compounds, BAZ2A crystallographic packing induced by stacking of compound **5**; electron density for compounds whose structure in complex with BAZ2 bromodomains has been described here.

DECLARATION OF INTEREST

The authors declare no competing financial interest.

ACKNOWLEDGMENTS

We thank the Structural Genomics Consortium at University of Oxford for providing the plasmids of the BAZ2 bromodomains and Oleg Fedorov for useful suggestions regarding the AlphaScreen setup. We are grateful to the staff at PXI beamline, Swiss Light Source, Paul Scherrer Institute (Villigen, Switzerland), and at XDR1 beamline, ELETTRA Synchrotron Light Source (Trieste, Italy), for on-site assistance. This work was supported financially by a grant from the Swiss National Science Foundation to A.C. (grant 31003A_169007). D.S. is a recipient of the SystemsX.ch translational postdoc fellowship and gratefully acknowledges support from the Holcim Foundation. G.L. is supported by a grant from the Associazione Italiana per la Ricerca sul Cancro (AIRC "MFAG 2017", code 19882).

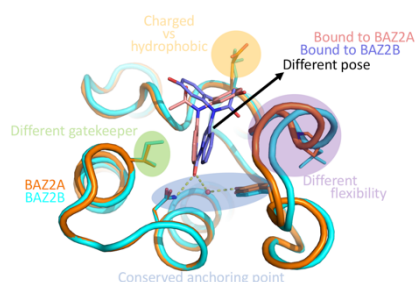
Keywords: BAZ2 bromodomains • protein X-ray crystallography • *in silico* screening • competition binding assay • prostate cancer

References:

- [1] Filippakopoulos P, Knapp S. Targeting bromodomains: epigenetic readers of lysine acetylation. *Nat. Rev. Drug Discov.* **2014**; 13:337-56.
- [2] Gu L, Frommel SC, Oakes CC, Simon R, Grupp K, Gerig CY, Bär D, Robinson MD, Baer C, Weiss M, Gu Z, Schapira M, Kuner R, Sültmann H, Provenzano M; ICGC Project on Early Onset Prostate Cancer, Yaspo ML, Brors B, Korb J, Schlömm T, Sauter G, Eils R, Plass C, Santoro R. BAZ2A (TIP5) is involved in epigenetic alterations in prostate cancer and its overexpression predicts disease recurrence. *Nat. Genet.* **2015**; 47:22-30.
- [3] Varambally S, Dhanasekaran SM, Zhou M, Barrette TR, Kumar-Sinha C, Sanda MG, Ghosh D, Pienta KJ, Sewalt RG, Otte AP, Rubin MA, Chinnaiyan AM. The polycomb group protein EZH2 is involved in progression of prostate cancer. *Nature* **2002**; 419:624-9.
- [4] <https://clinicaltrials.gov>
- [5] Arking DE, Junttila MJ, Goyette P, Huertas-Vazquez A, Eijgelsheim M, Blom MT, Newton-Cheh C, Reinier K, Teodorescu C, Uy-Evanado A, Carter-Monroe N, Kaikkonen KS, Kortelainen ML, Boucher G, Lagacé C, Moes A, Zhao X, Kolodgie F, Rivadeneira F, Hofman A, Witteman JC, Uitterlinden AG, Marsman RF, Pazoki R, Bardai A, Koster RW, Dehghan A, Hwang SJ, Bhatnagar P, Post W, Hilton G, Prineas RJ, Li M, Köttgen A, Ehret G, Boerwinkle E, Coresh J, Kao WH, Psaty BM, Tomaselli GF, Sotoodehnia N, Siscovick DS, Burke GL, Marbán E, Spooner PM, Cupples LA, Jui J, Gunson K, Kesäniemi YA, Wilde AA, Tardif JC, O'Donnell CJ, Bezzina CR, Virmani R, Stricker BH, Tan HL, Albert CM, Chakravarti A, Rioux JD, Huikuri HV, Chugh SS. Identification of a sudden cardiac death susceptibility locus at 2q24.2 through genome-wide association in European ancestry individuals. *PLoS Genet.* **2011**; 7:e1002158.
- [6] Ferguson FM, Fedorov O, Chaikuad A, Philpott M, Muniz JR, Felletar I, von Delft F, Heightman T, Knapp S, Abell C, Ciulli A. Targeting low-druggability bromodomains: fragment based screening and inhibitor design against the BAZ2B bromodomain. *J. Med. Chem.* **2013**; 56:10183-7.
- [7] Chen P, Chaikuad A, Bamborough P, Bantscheff M, Bountra C, Chung CW, Fedorov O, Grandi P, Jung D, Lesniak R, Linton M, Müller S, Philpott M, Prinjha R, Rogers C, Selenski C, Tallant C, Werner T, Willson TM, Knapp S, Drewry DH. Discovery and characterization of GSK2801, a selective chemical probe for the bromodomains BAZ2A and BAZ2B. *J. Med. Chem.* **2016**; 59:1410-24.
- [8] Drouin L, McGrath S, Vidler LR, Chaikuad A, Monteiro O, Tallant C, Philpott M, Rogers C, Fedorov O, Liu M, Akhtar W, Hayes A, Raynaud F, Müller S, Knapp S, Hoelder S. Structure enabled design of BAZ2-ICR, a chemical probe targeting the bromodomains of BAZ2A and BAZ2B. *J. Med. Chem.* **2015**; 58:2553-9.
- [9] Spiliotopoulos D, Wamhoff EC, Lolli G, Rademacher C, Caflisch A. Discovery of BAZ2A bromodomain ligands. *Eur. J. Med. Chem.* **2017**; 139:564-572.
- [10] Marchand JR, Lolli G, Caflisch A. Derivatives of 3-Amino-2-methylpyridine as BAZ2B Bromodomain Ligands: In Silico Discovery and in Crystallo Validation. *J. Med. Chem.* **2016**; 59:9919-9927.
- [11] Unzue A, Zhao H, Lolli G, Dong J, Zhu J, Zechner M, Dolbois A, Caflisch A, Nevado C. The "Gatekeeper" Residue Influences the Mode of Binding of Acetyl Indoles to Bromodomains. *J. Med. Chem.* **2016**; 59:3087-97.
- [12] Majeux N, Scarsi M, Apostolakis J, Ehrhardt C, Caflisch A. Exhaustive docking of molecular fragments with electrostatic solvation. *Proteins.* **1999**; 37:88-105.
- [13] Majeux N, Scarsi M, Caflisch A. Efficient electrostatic solvation model for protein-fragment docking. *Proteins.* **2001**; 42:256-68.
- [14] Spiliotopoulos D, Zhu J, Wamhoff EC, Deerrain N, Marchand JR, Aretz J, Rademacher C, Caflisch A. Virtual screen to NMR (VS2NMR): Discovery of fragment hits for the CBP bromodomain. *Bioorg. Med. Chem. Lett.* **2017**; 27:2472-78.
- [15] Crawford TD, Tsui V, Flynn EM, Wang S, Taylor AM, Cote A, Audia JE, Beresini MH, Burdick DJ, Cummings R, Dakin LA, Duplessis M, Good AC, Hewitt MC, Huang HR, Jayaram H, Kiefer JR, Jiang Y, Murray J, Nasveschuk CG, Pardo E, Poy F, Romero FA, Tang Y, Wang J, Xu Z, Zawadzke LE, Zhu X, Albrecht BK, Magnuson SR, Bellon S, Cochran AG. Diving into the Water: Inducible Binding Conformations for BRD4, TAF1(2), BRD9, and CECR2 Bromodomains. *J. Med. Chem.* **2016**; 59:5391-5402.
- [16] Tanaka M, Roberts JM, Seo HS, Souza A, Paulk J, Scott TG, De Angelo SL, Dhe-Paganon S, Bradner JE. Design and Characterization of Bivalent BET Inhibitors. *Nat. Chem. Biol.* **2016**; 12:1089-96.
- [17] Theodoulou NH, Bamborough P, Bannister AJ, Becher I, Bit RA, Che KH, Chung CW, Dittmann A, Drewes G, Drewry DH, Gordon L, Grandi P, Leveridge M, Linton M, Michon AM, Molnar J, Robson SC, Tomkinson NCO, Kouzarides T, Prinjha RK, Humphreys PG. Discovery of I-BRD9, a Selective Cell Active Chemical Probe for Bromodomain Containing Protein 9 Inhibition. *J. Med. Chem.* **2016**; 59:1425-1439.
- [18] Lolli G, Caflisch A. High-Throughput Fragment Docking into the BAZ2B Bromodomain: Efficient in Silico Screening for X-Ray Crystallography. *ACS Chem. Biol.* **2016**; 11:800-7.
- [19] Zhu J, Caflisch A. Twenty Crystal Structures of Bromodomain and PHD Finger Containing Protein 1 (BRPF1)/Ligand Complexes Reveal Conserved Binding Motifs and Rare Interactions. *J. Med. Chem.* **2016**; 59:5555-61.
- [20] Marchand JR, Caflisch A. Binding Mode of Acetylated Histones to Bromodomains: Variations on a Common Motif. *ChemMedChem.* **2015**; 10:1327-33.
- [21] Tallant C, Valentini E, Fedorov O, Overvoorde L, Ferguson FM, Filippakopoulos P, Svergun DI, Knapp S, Ciulli A. Molecular basis of histone tail recognition by human TIP5 PHD finger and bromodomain of the chromatin remodeling complex NoRC. *Structure.* **2015**; 23:80-92.
- [22] Landrum G. RDKit: Open-source cheminformatics. rdkit.org
- [23] Vanommeslaeghe K, MacKerell AD Jr. Automation of the CHARMM General Force Field (CGenFF) I: Bond Perception and Atom Typing. *J. Chem. Inf. Model.* **2012**; 52:3144-54.
- [24] Vanommeslaeghe K, Raman EP, MacKerell AD Jr. Automation of the CHARMM General Force Field (CGenFF) II: Assignment of Bonded Parameters and Partial Atomic Charges. *J. Chem. Inf. Model.* **2012**; 52:3155-68.
- [25] Scarsi M, Apostolakis J, Caflisch A. Continuum electrostatic energies of macromolecules in aqueous solutions. *J. Phys. Chem. A* **1997**; 101:8098-8106.
- [26] Philpott M, Yang J, Tumber T, Fedorov O, Uttarkar S, Filippakopoulos P, Picard S, Keates T, Felletar I, Ciulli A, Knapp S, Heightman TD. Bromodomain-peptide displacement assays for interactome mapping and inhibitor discovery. *Mol. Biosyst.* **2011**; 7:2899-908.
- [27] D'Agostino VG, Lal P, Mantelli B, Tiedje C, Zucal C, Thongon N, Gaestel M, Latorre E, Marinelli L, Seneci P, Amadio M, Provenzano A. Dihydroanthranone-I interferes with the RNA-binding activity of HuR affecting its post-transcriptional function. *Sci. Rep.* **2015**; 5:16478.
- [28] Quinn E, Wodicka L, Ciceri P, Pallares G, Pickle E, Torrey A, et al. BROMOscan - a high throughput, quantitative ligand binding platform identifies best-in-class bromodomain inhibitors from a screen of mature compounds targeting other protein classes. *Cancer Res.*

- 2013**; 73:4238.
- [29] Marchand JR, Dalle Vedove A, Lolli G, Cafisch A. Discovery of Inhibitors of Four Bromodomains by Fragment-Anchored Ligand Docking. *J. Chem. Inf. Model.* **2017**; 57:2584-97.
- [30] Lolli G, Battistutta R. Different orientations of low-molecular-weight fragments in the binding pocket of a BRD4 bromodomain. *Acta Crystallogr. D Biol. Crystallogr.* **2013**; 69:2161-4.
- [31] Kabsch W. Xds. *Acta Crystallogr. D Biol. Crystallogr.* **2010**; 66:125-32.
- [32] Evans PR, Murshudov GN. How good are my data and what is the resolution? *Acta Crystallogr. D Biol. Crystallogr.* **2013**; 69:1204-14.
- [33] Karplus PA, Diederichs K. Assessing and maximizing data quality in macromolecular crystallography. *Curr. Opin. Struct. Biol.* **2015**; 34:60-8.
- [34] McCoy AJ, Grosse-Kunstleve RW, Adams PD, Winn MD, Storoni LC, Read RJ. Phaser crystallographic software. *J. Appl. Crystallogr.* **2007**; 40:658-74.
- [35] Adams PD, Afonine PV, Bunkoczi G, Chen VB, Davis IW, Echols N, Headd JJ, Hung LW, Kapral GJ, Grosse-Kunstleve RW, McCoy AJ, Moriarty NW, Oeffner R, Read RJ, Richardson DC, Richardson JS, Terwilliger TC, Zwart PH. PHENIX: a comprehensive Python-based system for macromolecular structure solution. *Acta Crystallogr. D Biol. Crystallogr.* **2010**; 66:213-21.
- [36] Emsley P, Lohkamp B, Scott WG, Cowtan K. Features and development of Coot. *Acta Crystallogr. D Biol. Crystallogr.* **2010**; 66:486-501.

Entry for the Table of Contents



Very limited differences can be identified in the Kac binding pockets of BAZ2A and BAZ2B bromodomains, which are however sufficient to determine different poses for the bound inhibitors and could be exploited for the design of selective inhibitors.